

Experimental Determination of Surface Stress Changes in Electrochemical Systems – Possibilities and Pitfalls

G. G. Láng,* N. S. Sas, and S. Vesztergom

Eötvös Loránd University, Institute of Chemistry,
Department of Physical Chemistry,
H-1117 Budapest, Pázmány P. s. 1/A

Original scientific paper
Received: July 26, 2008
Accepted: August 4, 2008

In the present paper, the different techniques used for the determination of changes of surface stress of solid electrodes, as well as the kind and quality of information that can be achieved using these methods are discussed. The most important methods are briefly reviewed and advantages/drawbacks highlighted. Special attention is paid to issues related to the use of the “bending beam” (“bending cantilever”, “laser beam deflection”, “wafer curvature”, etc.) methods. Recent development in these techniques has been introduced and discussed.

Key words:

Electrochemical system, surface stress, surface tension, solid/liquid interface, solid electrode

Introduction

The surface stress (“surface tension”) or the “specific surface energy” (“generalized surface parameter”¹) of solid electrodes is an important physical quantity, since most electrochemical systems involving solids are, in fact, capillary systems, because any interaction between the bulk solid and the remainder of the system takes place via the surface region. Since thermodynamic properties of the surface region directly influence the electrochemical processes, an understanding of the thermodynamics of solid surfaces is of importance to all surface scientists and electrochemists.

Unfortunately, for solid electrodes the thermodynamic interpretation of the results from various methods in terms of physicochemical properties of the system is not without problems.^{2–20} In principle, the results of the theoretical work can be checked experimentally; however, specific surface energies of solid/liquid interfaces are very difficult to measure owing to the lack of reliable and sensitive methods. Theoretical estimates of absolute surface tension of some relatively simple covalently bonded, ionic, rare-gas, and metallic crystals are discussed in the literature.²¹ In a few specific situations, the surface tensions of some solid surfaces have been determined experimentally. These experimental methods are designed for the solid/gas interface, and are mostly incompatible for use at room temperature or in the presence of an electrolyte solution. Consequently, they cannot be applied to study the surface energetics of solid electrodes.

It is not surprising therefore, that during the past decades several attempts have been made to derive thermodynamic equations for the solid/liquid interface, and several methods were suggested for measurements of *changes* of the surface stress of solid electrodes.^{22–32}

Attempts to determine the surface stress of solid electrodes fall into two main categories: measurement of the potential dependence of contact angle established by liquid phase on the solid surface and the measurement of the variation in surface stress experienced by the solid as a function of potential. Variation in the stress may either be measured “directly”,^{23,33,34} with a piezoelectric element, or be obtained indirectly,^{30,35–39} by measuring the potential dependence of the strain (i.e. electrode deformation) and then obtaining the variation in stress from the appropriate form of Hooke’s law. It should be stressed again that the above methods only yield changes of surface stress as a function of various physicochemical parameters e.g. as a function of electrode potential, and in principle, if there are both “plastic” and “elastic” contributions to the total strain, the changes of the “generalized surface parameter”¹ can be determined.

Unfortunately, most of the proposed methods have drawbacks; i.e., they are technically demanding, they cannot be used to monitor changes of the surface stress, they are semiempirical and depend on further assumptions, or they are not generally applicable.

This paper discusses the different techniques used for the determination of changes of surface stress of electrodes (“bending beam” method [e.g.^{24–32,40}], interferometry [e.g.^{36,39,41–43}], piezo-

*Corresponding author. Tel.: +36 1 209 0555/1107;
fax: +36 1 372 2592. E-mail: langgyg@chem.elte.hu

electric method [e.g.^{44–46}], extensometer method [e.g.^{47,48}], as well as the kind and quality of information that can be achieved using these methods. Special attention has been paid to problems related to the use of the “bending beam” (“bending cantilever”, “laser beam deflection”, “wafer curvature”) method.

Experimental methods

Piezoelectric method

According to our knowledge, Gokhshtein^{49–51} was the first to measure changes $\partial\gamma_s/\partial E$ of the surface stress γ_s with the electrode potential E at platinum electrodes in sulfuric acid using the “piezoelectric” method. The piezoelectric method originally developed by Gokhshtein³³ and improved by various authors,^{34,44,52,53} especially by Seo *et al.*,^{34,53} is a very powerful in-situ method for the rapid determination of surface energy changes. The method is “direct” in the sense that it is the variation in the electrode deformation that is “registered” directly by a piezoelectric element. A metal plate is rigidly connected, in a special manner, to a highly sensitive piezoelectric element (Fig. 1). The applied potential consists of a mean component upon which is superimposed a high-frequency component. Electrode potential oscillations with an amplitude ΔE will result in oscillations with an amplitude $\Delta\gamma_s$ in the surface stress, which in turn set up forces of inertia that excite vibrations in the entire electrode-piezoelement unit. By applying this method $\partial\gamma_s/\partial E$ is measured at high frequencies and the quantitative determination of surface energy changes requires a difficult calibration procedure (the transfer function of the mechanical coupling is rather complicated). However, the potentials of

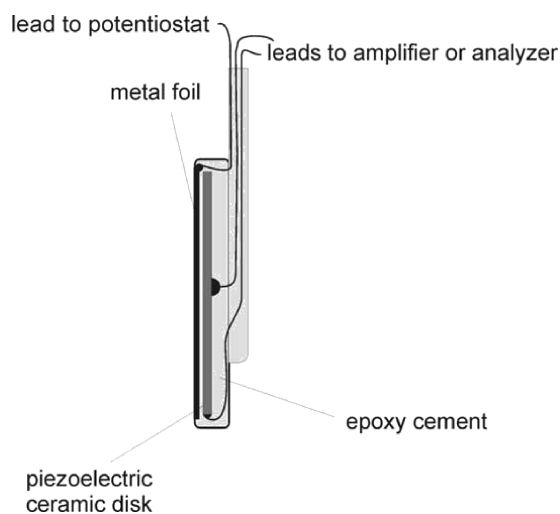


Fig. 1 – Schematic illustration of a device for the “piezoelectric method”

extrema of the function surface stress vs. potential can be obtained directly. A series of measurements has been performed to date in order to understand electrode processes such as electrosorption and initial oxidation. This technique was capable of detecting sensitively the shift in potential of zero charge (pzc) due to the adsorption of ions and the sign reversal of surface charge due to the formation and reduction of surface oxide phases. E.g. in case of platinum in sulphuric acid solutions Gokhshtein observed two extrema in the hydrogen adsorption region.³⁰ Similar results were obtained by Seo *et al.*³⁴ applying the same experimental method to platinum in 0.5 M acid sulfate solutions. On the other hand, Malpas *et al.*⁴⁴ observed only one extremum at $E \approx 0.05$ V for platinum in 0.1 M sulfuric acid. The electrode potential of the maximum was found to shift with pH to more negative values according to $\partial E_m/\partial \text{pH} = -40$ mV.³⁴

Obviously, because of the dynamic features of the method, the recorded variation in surface stress does not always correspond to equilibrium conditions. In addition, as indicated above, the greatest disadvantage of the method is that the surface energy change can be calculated from the measured signal only after a sophisticated calibration procedure.

The extensometer method

Beck *et al.*^{47,54,55} attempted to determine variations in surface stress as a function of potential by using an extensometer which measures the corresponding variation in the length of a very thin metal ribbon. (The results published more recently in ref. [56] are also noteworthy.) The variation in surface stress, $\Delta\gamma_s$, can be obtained from the change in the ribbon length ΔL by an equation developed by Beck:

$$\Delta\gamma_s = -\frac{AE}{PL} \Delta L \quad (1)$$

where A and P are the cross-sectional area and periphery of the ribbon and E is Young’s modulus (Fig. 2).

Unfortunately, thermal expansion constitutes a serious problem in the extensometer method. The error due to thermal expansion can be reduced, but unless the effect on thermal expansion can be quantitatively accounted for, the results of the extensometer method cannot be conclusively interpreted.

The “bending beam” method

The principles of the “bending beam” (“bending cantilever”, “laser beam deflection”, “wafer curvature”, etc.) method were first stated by Stoney,^{57,58} who derived an equation relating the

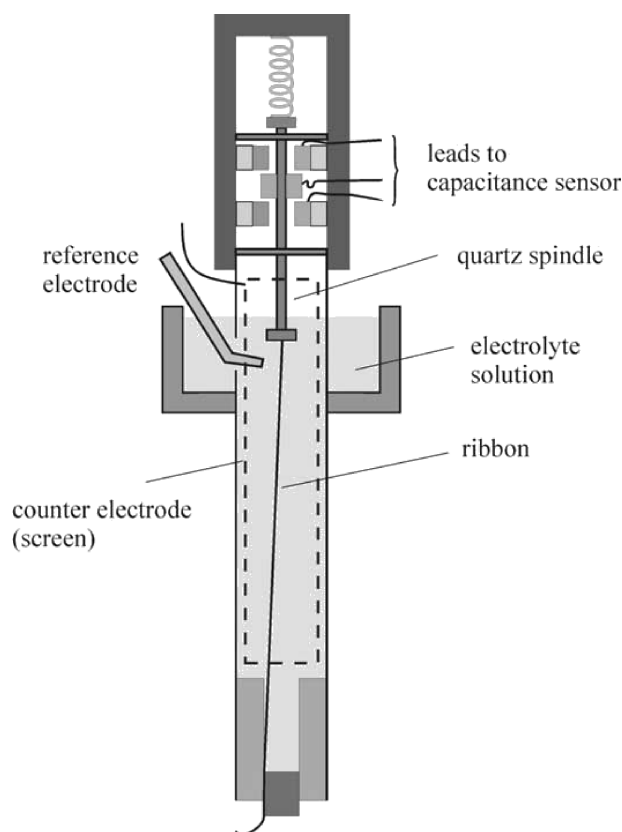


Fig. 2 – Design of the extensometer

stress in the film to the radius of curvature of the beam.

Measuring the bending of a plate or strip to determine surface stress change or the stress in thin films is a common technique, even in electrochemistry.^{22–32} It has been also used for instance for the investigation of the origin of electrochemical oscillations at silicon electrodes⁵⁹ or in the course of galvanostatic oxidation of organic compounds on platinum,^{39,40} for the study of volume changes in polymers during redox processes,⁶⁰ for the investigation of the response kinetics of the bending of polyelectrolyte membrane platinum composites by electric stimuli,⁶¹ and for the experimental verification of the adequacy of the “brush model” of polymer modified electrodes,⁶² etc.

The “bending beam” method can be effectively used in electrochemical experiments, since the changes of the surface stress ($\Delta\gamma_s$) for a thin metal film on one side of an insulator (e.g. glass) strip (or a metal plate, one side of which is coated with an insulator layer) in contact with an electrolyte solution can be estimated from the changes of the radius of curvature of the strip. If the potential of the electrode changes, electrochemical processes resulting in the change of γ_s can take place exclusively on

the metal side of the sample. The change in γ_s induces a bending moment and the strip bends. In case of a thin metal film on a substrate if the thickness of the film t_f is sufficiently smaller than the thickness of the plate, $t_s \gg t_f$, the change of γ_s can be obtained by an expression based on a generalized form of Stoney’s equation⁵⁷

$$\Delta\gamma_s = k_i \Delta(1/R) \quad (2)$$

where k_i depends on the design of the electrode. In most cases

$$k_i = \frac{E_s t_s^2}{6(1 - \nu_s)} \quad (3)$$

where E_s , ν_s , and R are Young’s modulus, Poisson’s ratio and radius of curvature of the plate, respectively.

The derivation of eqs. (2) and (3) imply the assumption that $\Delta\gamma_s = t_f \Delta g_f$, where Δg_f is the change of the film stress. (In principle, if there are both plastic and elastic contributions to the total strain, the change of the “generalized surface parameter” ($\Delta\gamma_s$)¹ can be determined.) According to eq. (2), for the calculation of $\Delta\gamma_s$ the changes of the reciprocal radius $\Delta(1/R)$ of curvature of the plate must be known.

The values of $\Delta(1/R) = \Delta\gamma_s/k_i$ can be calculated,

a) if the changes of the deflection angle of a laser beam mirrored by the metal layer on the plate are measured using an appropriate experimental setup as shown in Fig. 3,

b) or the deflection of the plate is determined directly, e.g. with a scanning tunneling microscope.

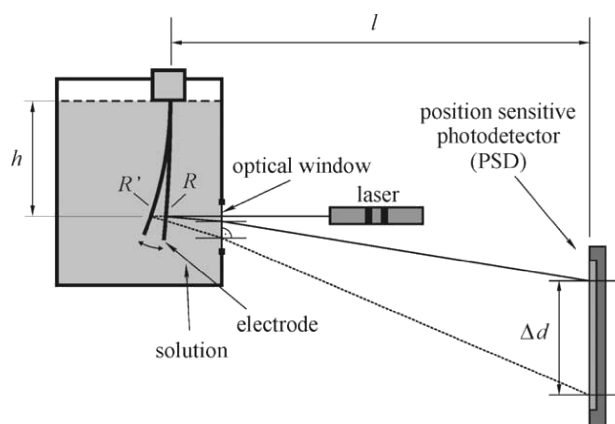


Fig. 3 – Scheme of the electrochemical (optical) bending beam setup. Δd : the displacement of the light spot on the position sensitive detector if the radius of curvature changes from R to R' . l : the distance between the electrode and the photodetector; h : the distance between the solution level and the reflection point.

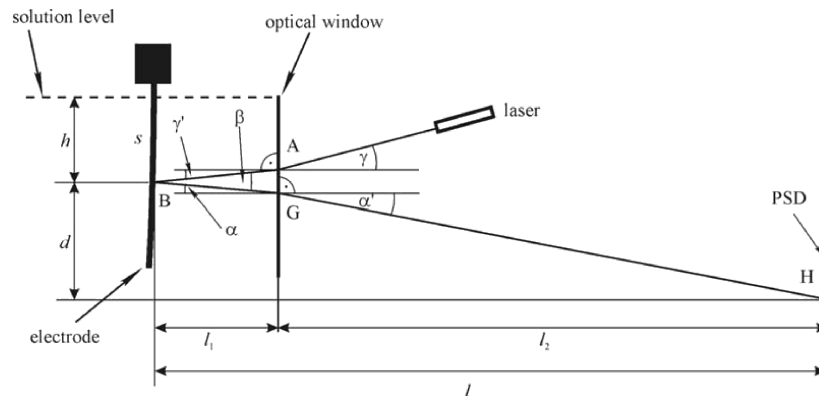


Fig. 4 – Optical configuration of a typical arrangement for electrochemical bending beam experiments. γ : the angle of incidence of the light beam coming directly from the laser (in air), γ' : the angle of refraction at A, α : angle of incidence at G, α' : angle of refraction at G, H: light spot at H on the detector plane, l : the distance between the electrode and the photodetector, l_1 : the distance between the optical window and the reflection point (B) on the electrode, l_2 : the distance between the optical window and the position sensitive detector (PSD), s : the length of the electrode in the solution, h : the distance between the solution level and the reflection point.

Optical detection

Direct position sensing

Fig. 4 shows a possible arrangement for electrochemical bending beam experiments with optical detection.⁶³ Such a setup can be used mainly for the investigation of small deflections, and several details may be different in special cases. E.g. a multi-beam optical technique was used by Proost *et. al* in.^{64,65} With this technique, the spacings between a one-dimensional array of multiple laser reflections off the cantilevered substrate can be continuously monitored with a charge coupled device (CCD) camera.

As it can be seen in Fig. 4, l is the distance between the electrode and the photodetector, l_1 is the distance between the optical window and the reflection point (B) on the electrode, l_2 is the distance between the optical window and the detector plane, and s is the length of the electrode in the solution, respectively. The angle of incidence of the light beam coming directly from the laser (in air) is γ . Because of the refraction at A the direction of the beam changes, the new direction of it (in the solution) is AB, the angle of refraction is γ' . The laser beam arriving from the direction AB is reflected at point B on the surface. The direction of the reflected beam (which strikes the surface of the optical window with an angle of incidence of α) is BG. Due to the refraction at G, the direction of the reflected beam changes again, the new direction of it (in air) is GH, and the angle of refraction is α' . The reflected beam results in a light spot at H on the detector plane. According to the above considerations, if the radius of curvature of the electrode changes, a

displacement of the light spot (Δd) on the position sensitive detector can be observed.

The distance d can be expressed with the help of the corresponding triangles:

$$d = l_1 \tan \alpha + l_2 \tan \alpha' \quad (4)$$

and

$$l_1 + l_2 = l \quad (5)$$

From Fig. 4 and from Fig. 5 (in which the corresponding segment of the electrode with the incident and reflected light beam is magnified) we can see that

$$\alpha + \gamma' = \beta, \quad (6)$$

and

$$\frac{\beta}{2} = 90^\circ - (\varepsilon - \gamma'). \quad (7)$$

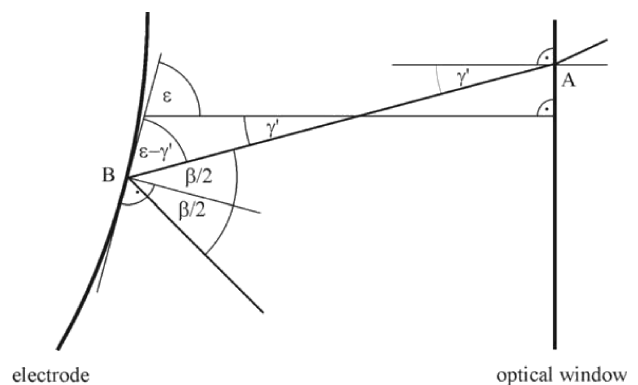


Fig. 5 – A magnified segment of the electrode with the incident and reflected light beam (see Fig. 4)

Taking into account the rectangle triangle shown in Fig. 5 the angle δ can be expressed as

$$\delta = 90^\circ - \varepsilon \quad (8)$$

By combining eqs. (6)–(8) one obtains

$$\alpha = 2\delta + \gamma' \quad (9)$$

To express α' , which is the angle between the normal to the optical window and the light beam exiting the electrochemical cell, we can use Schnell's law:

$$\frac{\sin \alpha'}{\sin \alpha} = n_s \quad (10)$$

From eq. (4) we have:

$$d = l_1 \tan \alpha + l_2 \frac{\sin \alpha'}{\sqrt{1 - \sin^2 \alpha'}} \quad (11)$$

and, with eqs. (9) and (10)

$$d = l_1 \tan(2\delta + \gamma') + l_2 n_s \frac{\sin(2\delta + \gamma')}{\sqrt{1 - n_s^2 \sin^2(2\delta + \gamma')}} \quad (12)$$

It can be seen, that eq. (12) is suitable (at least in principle) for calculating d using experimentally measurable parameters: the values of δ and γ' can be determined knowing the incident angle of the beam, the refractive index and the radius of curvature of the plate.

However, on the basis of this expression we can derive simpler equations for the change in d when δ changes. Differentiating the $d(\delta)$ function with respect to δ we have:

$$\frac{dd}{d\delta} = 2l_1 \frac{1}{\cos^2(2\delta + \gamma')} + 2l_2 n_s \frac{\cos(2\delta + \gamma')}{[1 - n_s^2 \sin^2(2\delta + \gamma')]^{3/2}} \quad (13)$$

By taking into account eqs. (9) and (10), eq. (13) can be rewritten into a simpler form, from which it is clear that the factor multiplying n_s in the second term of the RHS of eq. (13) is always greater than one:

$$\frac{dd}{d\delta} = 2l_1 \frac{1}{\cos^2 \alpha} + 2l_2 n_s \frac{\cos \alpha}{\cos^3 \alpha'} \quad (14)$$

It is clear that $\alpha' \geq \alpha$, since the solution is the optically denser medium. However, from $\alpha' \geq \alpha$ follows that $\cos^3 \alpha' \leq \cos \alpha' \leq \cos \alpha \leq 1$, and therefore

$$\frac{\cos \alpha}{\cos^3 \alpha'} \geq 1 \quad (15)$$

Since $dd = sd(1/R)$, by using eq. (13) the following equation can be obtained:

$$\frac{dd}{d(1/R)} = 2sl_1 \frac{1}{\cos^2\left(\frac{2s}{R} + \gamma'\right)} + 2sl_2 n_s \frac{\cos\left(\frac{2s}{R} + \gamma'\right)}{\left[1 - n_s^2 \sin^2\left(\frac{2s}{R} + \gamma'\right)\right]^{3/2}} \quad (16)$$

It should be noted, that except for the assumption that the thickness of the optical window is zero (see later), no approximations were used in the derivation of eq. (16).

Now we can express Δd (the change of the position of the light spot on the PSD) by using Schnell's law ($\frac{\sin \gamma}{\sin \gamma'} = n_s$) and the following assumptions: $\Delta(1/R)$ is small enough to use first-order approximation for the changes, $s \approx h$, and $2s/R = 2\delta \ll \gamma'$.

According to the above considerations:

$$\Delta d \approx \frac{dd}{d(1/R)} \Delta(1/R) \approx \left[2hl_1 \frac{1}{1 - n_s^{-2} \sin^2 \gamma} + 2hl_2 n_s \frac{(1 - n_s^{-2} \sin^2 \gamma)^{1/2}}{(1 - \sin^2 \gamma)^{3/2}} \right] \Delta(1/R) \quad (17)$$

In addition, if $l_1 \ll l_2$.

$$\Delta d \approx 2lh n_s \left[\frac{(1 - n_s^{-2} \sin^2 \gamma)^{1/2}}{(1 - \sin^2 \gamma)^{3/2}} \right] \Delta(1/R) \quad (18)$$

or

$$\Delta(1/R) \approx \frac{\Delta d}{2lh n_s} \left[\frac{(1 - \sin^2 \gamma)^{3/2}}{(1 - n_s^{-2} \sin^2 \gamma)^{1/2}} \right] = \frac{\Delta d}{2lh n_s} \xi(\gamma, n_s) \quad (19)$$

The factor $\xi(\gamma, n_s)$ in square brackets in eq. (19), expressing the effect of the incident angle, is a monotonously decreasing function of γ , and for $n_s(20^\circ \text{C}) \approx 1.33$ (pure water) and for $\gamma = 10^\circ$ it has the value of $\xi(10^\circ, 1.33) = 0.966$, the value of $\xi(30^\circ, 1.33) = 0.721$ for $n_s(20^\circ \text{C}) \approx 1.33$ and $\gamma = 30^\circ$; $\xi(10^\circ, 1.42) = 0.965$ for $\gamma = 10^\circ$ and $n_s(20^\circ \text{C}) \approx 1.42$ (this is the refractive index e.g. of propylene carbonate), and $\xi(30^\circ, 1.42) = 0.716$ for $\gamma = 30^\circ$ and

$n_s(20\text{ }^\circ\text{C}) \approx 1.42$, respectively. Note that if the deflection of the electrode is small and γ tends to zero (“normal incidence”) we get back the formula derived earlier for perpendicular incident light:⁶⁶

$$\Delta d \approx 2lh n_s \Delta(1/R) \quad (20)$$

or

$$\Delta(1/R) \approx \frac{\Delta d}{2lh n_s} \quad (21)$$

As it can be seen from eqs. (2), (3), and (21) if the actual values of k_i (or t_s , E_s , ν_s), l , h , and n_s are known, for the calculation of $\Delta\gamma_s$ only the experimental determination of Δd is necessary.

Unfortunately, in many papers reporting results on electrochemical bending beam experiments with optical detection, schemes of experimental arrangements can be found in which the direction of the reflected beam before and after passing the optical window or the air/solution boundary is indicated incorrectly, since the effect of refraction is ignored (see e.g. in ^{63,66,67}). It is even more regrettable that the effect of refraction is often neglected also in the calculations. In addition no reference is made to the refractive index of the solution, or the value of the refractive index of the solution is not indicated. However, refractive indices of aqueous solutions are about 1.33 – 1.48. It is evident from the above equations that the complete neglect of the bending of the laser beam due to refraction at the optical window may cause an error of about 25–32 % in the determination of $\Delta\gamma_s$ in aqueous solutions (because of n_s only!), and the error is more pronounced in the case of liquids of higher refractive index. The error is even greater (e.g., it is about 50 % for $n_s = 1.42$ and $\gamma = 30^\circ$) if the incident angle is different from zero.

Another source of errors is associated with the “shifting” due to the thickness of the optical window.⁶⁸ Nevertheless, this effect is expected to be negligible for aqueous solutions and glass optical windows.

Interferometric detection

The deflection of a strip or a plate can also be measured interferometrically. Fig. 6 shows the principle of the electrochemical Kösters laser interferometer, which can be used for the determination of changes of surface stress by the resulting deformation of an elastic plate. The Kösters laser interferometer (Kösters-prism⁶⁹ interferometer) is a laser-illuminated double-beam interferometer. The main advantage of this type of interferometer is its high immunity to environmental noise due to the close vicinity of the two interfering beams. This immu-

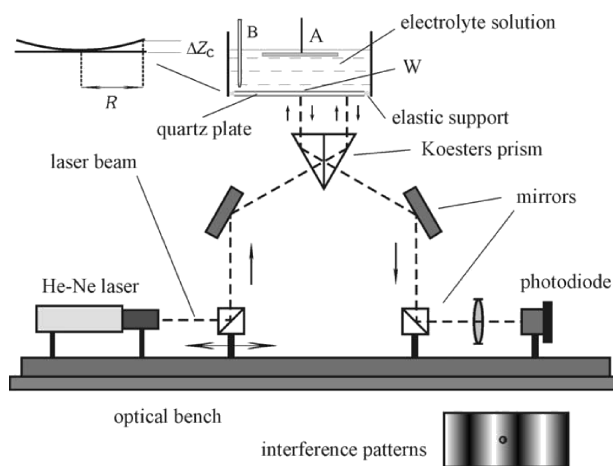


Fig. 6 – Interferometric apparatus with He-Ne laser and Kösters prism. W: working electrode; A: counter electrode; B: reference electrode.

nity makes it an ideal tool for high-precision measurements. The central constituent of the interferometer is the Kösters-prism beam splitter, which produces two parallel coherent beams. The two reflected beams recombine in the prism, and an interference pattern can be observed. Kösters-prisms consist of two identical prism halves which are cemented together. The angles of the prism halves are 30° – 60° – 90° , with high angular accuracy, and one long cathetus side is semi-transparent (the reflection and transmission coefficients are equal).

As it can be seen in Fig. 6, the light beam is reflected by the metal mirror perpendicular to the entrance side of the prism. The point of entrance determines the distance of the two beams emerging from the base of the prism. They are reflected at a nearly zero angle of incidence from the plate. The interfering light leaves the Kösters prism through the exit side, and it is projected onto a screen with a hole of a given diameter and a photodiode behind it. The difference between the optical path lengths ($2 \times \Delta Z_C$) can be determined from the change in light intensity detected by the photodiode. The height ΔZ_C of the center of the plate with respect to a plane at a given radius yields $\Delta\gamma_s$ from the appropriate form of Hooke's law

$$\Delta\gamma_s = k\Delta Z_C \quad (22)$$

The sensitivity is of the order 0.1 nm with respect to ΔZ_C and 1 mN m^{-1} with respect to $\Delta\gamma_s$. The constant k in eq. (22) is determined by the mechanical properties of the quartz plate (radius R) and by the type and quality of the support at the edge of the plate.

Choosing a circular AT-cut quartz plate with a thin metal layer on it in contact with the solution being the working electrode in an electrochemical

cell provides the advantage to measure simultaneously surface energy, mass and charge.^{36,39,41–43,70} (If the metal layers on both sides of the quartz disc are connected to an appropriate oscillator circuit, the device can be used as an electrochemical quartz crystal microbalance.) In addition, since the light beams do not pass the air/solution interface, the effects of light refraction at the surface are excluded.

Even though there are great advantages of the interferometric detection, there are still some problems connected with this method. As mentioned above the type and quality of the support at the edge of the plate is extremely important. The shape and the magnitude of the deformation $Z(r, \varphi)$ as a function of the radial distance r and the angle φ depends on the type of support at the edge of the circular plate. The largest deformation and thus the highest sensitivity for measurements of the surface stress change is expected for the “unsupported” plate. A plate is also unsupported if a mounting is present but exerts no forces on the edge. Evidently, the design and realization of such a device is very difficult.³⁶ In addition, no absolutely satisfactory solution has been found for the problem of making reliable electrical connections to the metal layers on the quartz crystal. In the case of evaporated/sputtered metal layers the high surface stress changes may cause problems with the adhesion of the films, etc.

Detection by microscopy

A rather elegant method to measure the bending of a strip or a plate is to use the scanning tunneling microscope (STM).^{37,71–75} The STM may be used then as a means to simultaneously investigate the structure of the surface (Fig. 7). (It should be noted that the atomic force microscope (AFM), is a

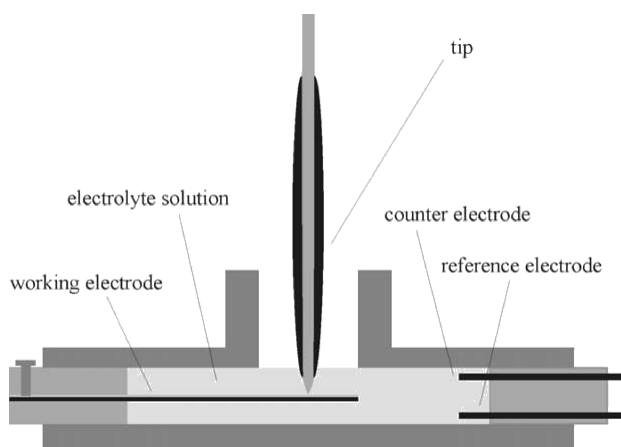


Fig. 7 – Schematic illustration of a typical arrangement for STM studies at the solid/liquid interface which allows simultaneously to measure the bending of the cantilever when the electrode potential is varied

combination of the principles of the scanning tunneling microscope and the stylus profilometer (SP), where the stylus in the profilometer is carried by a cantilever beam and it rides on the sample surface.⁷⁶)

However, even this method is not without pitfalls. In electrolyte solutions there is double layer like structure also around the STM tip. Consequently, there are some interactions between the tip of the STM and the sample that seem to be unavoidable. These are: long range electrostatic interactions between electrical (electrochemical) double layers, and structural/dispersion/hydration forces that dominate the interaction at very short ranges. Most of these contributions have been widely studied but some are marginally understood. The repulsion of two double layers was discussed e.g. in [77–80]. As it has been noted in [81] “... one can lift solids by the electrical forces in the double layer”. We note here that attractive forces were observed also between two gold spheres used in vacuum tunneling.⁸²

In experiments reported in [75] a small circular portion of the liquid was removed by a syringe in the vicinity of the tip (Fig. 8). According to the authors with this simple procedure the tip remained dry and the electrochemical offset current with its concomitant noise was eliminated. The values of the surface stress changes derived from the Stoney formula were corrected for the small area not covered by the solution. The uncertainty incurred by this procedure has been estimated at most 5 %. Obviously, in this setup the error due to the interaction between double layers is eliminated, but a new source of error, namely that due to the creation of a three phase boundary, is introduced (Fig. 8). It is well known, that in a three-phase system there is a greater likelihood of surface contamination from organic and oxygen impurities present in the gas

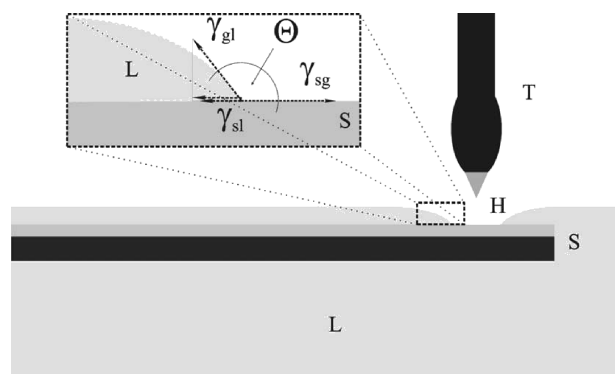


Fig. 8 – A bending cantilever setup with a “hole” in the liquid layer at the vicinity of the STM tip. L: electrolyte solution, S: cantilever sample, H: hole, T: STM tip, Θ : contact angle. γ_{sg} , γ_{sl} and γ_{gl} are the surface tension at the solid-gas, solid-liquid, and liquid-gas interfaces, respectively.

phase. On the other hand, the wetting of such metals as gold and platinum is still a subject of controversy among those who consider these metals to be hydrophobic in nature and others who report low or zero contact angle. It is clear, that if the surface tension of the liquid-gas interface or/and the contact angle changes during the experiment, the results obtained may be incorrect.

As pointed out in [22], another source of error, which can be important, arises because the exact elastic behavior of membranes is strongly dependent on the boundary conditions, which are not well defined in many experiments. E.g. in the study reported in ref. [71], the bending of a crystal disc was measured. This disc was clamped on the entire circular boundary. For a flat disc which is clamped on the perimeter, a bending in either direction increases the area of both surfaces (Fig. 9). Consequently, a tensile stress applied to either surface would not bend the plate at all.²² In reality, a disc or a plate is always slightly deformed and one would, therefore, observe also a linear effect on such a sample. However, the magnitude of the bending effect would depend on the initial bending of the crystal.

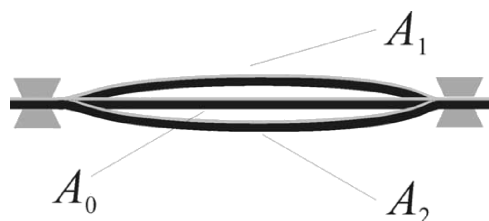


Fig. 9 – The bending of a rigidly clamped plate. Bending to either side enlarges the area of both surfaces. A_0 : surface area without bending; A_1, A_2 : surface area of the deformed sample. Obviously, $A_1, A_2 > A_0$.

Conclusions

In their famous textbook ‘*Electrochemical Methods*’ A. J. Bard and L. R. Faulkner wrote in 1980 that “Examining interfacial structure at a solid surface is extremely difficult ... Measurements of surface tension and surface stress are not easy, but a great deal of attention has been paid to them recently; and there is reason for optimism about the future in this area”.⁸³ In retrospect, this prediction did not exactly come true, however, promising results have been obtained in this field. Especially, the “bending beam” or “bending plate” (“bending cantilever”, “laser beam deflection”, “wafer curvature”, etc.) methods with optical detection (PSD or interferometer) seem to be generally applicable. However, even these methods are not without potential problems. It is necessary to be flexible and

to choose the most appropriate method for each particular case. We hope that this short review will help the interested reader to select the most appropriate technique for a given problem.

ACKNOWLEDGEMENT

Financial support by the Hungarian Scientific Research Fund (OTKA K045888, OTKA K67994) is gratefully acknowledged.

References

1. Trasatti, S., Parsons, R., *Pure & Appl. Chem.* **58** (1986) 437.
2. Linford, R. G., *Chem. Rev.* **78** (1978) 81.
3. Láng, G., Heusler, K. E., *Journal of Electroanalytical Chemistry* **377** (1994) 1.
4. Heusler, K. E., Láng, G., *Electrochimica Acta* **42** (1997) 747.
5. Guidelli, R., *J. Electroanal. Chem.* **453** (1998) 69.
6. Láng, G., Heusler, K. E., *J. Electroanal. Chem.* **472** (1999) 168.
7. Guidelli, R., *J. Electroanal. Chem.* **472** (1999) 174.
8. Valincius, G., *J. Electroanal. Chem.* **478** (1999) 40.
9. Lipkowski, J., Smickler, W., Kolb, D. M., Parsons, R., *J. Electroanal. Chem.* **452** (1998) 193.
10. Couchman, P. R., Jesser, W. A., Kuhlmann-Wilsdorf, D., *Surf. Sci.* **33** (1972) 429.
11. Couchman, P. R., Jesser, W. A., *Surf. Sci.* **34** (1973) 212.
12. Couchman, P. R., Everett, D. W., Jesser, W. A., *J. Colloid Interface Sci.* **52** (1975) 410.
13. Rusanov, A. I., *J. Coll. Interf. Sci.* **63** (1978) 330.
14. Rusanov, A. I., *Pure&Appl. Chem.* **61** (1989) 1945.
15. Rusanov, A. I., *Surf. Sci. Rep.* **23** (1996) 173.
16. Everett, D. W., Couchman, P. R., *J. Electroanal. Chem.* **67** (1976) 382.
17. Grafov, B. M., Paasch, G., Plieth, W., Bund, A., *Electrochim. Acta* **48** (2003) 581.
18. Marichev, V. A., *Surf. Sci.* **600** (2006) 4527.
19. Marichev, V. A., *Chem. Phys. Lett.* **434** (2007) 218.
20. Marichev, V. A., *Prot. Met.* **44** (2008) 105.
21. Bikerman, J. J., in *Topics in Current Chemistry*; 77, Springer-Verlag, Berlin, 1978.
22. Ibach, H., *Surf. Sci. Reports* **29** (1997) 193.
23. Ueno, K., Seo, M., *J. Electrochem. Soc.* **146** (1999) 1496.
24. Fredlein, R. A., Damjanovic, A., Bockris, J. O'M., *Surf. Sci.* **25** (1971) 261.
25. Fredlein, R. A., Bockris, J. O'M., *Surf. Sci.* **46** (1974) 641.
26. Sahu, S. N., Scarminio, J., Decker, F., *J. Electrochem. Soc.* **137** (1990) 1151.
27. Tian, F., Pei, J. H., Hedden, D. L., Brown, G. M., Thundat, T., *Ultramicroscopy* **100** (2004) 217.
28. Cattarin, S., Pantano, E., Decker, F., *Electrochem. Commun.* **1** (1999) 483.
29. Cattarin, S., Decker, F., Dini, D., Margesin, B., *J. Electroanal. Chem.* **474** (1999) 182.
30. Raiteri, R., Butt, H.-J., Grattarola, M., *Scanning Microscopy* **12** (1998) 243.
31. Kongstein, O. E., Bertocci, U., Stafford, G. R., *J. Electrochem. Soc.* **152** (2005) C116.

32. *Stafford, G. R., Bertocci, U.*, *J. Phys. Chem. B* **110** (2006) 15493.
33. *Gokhshtein, A. Ya.*, in “Surface Tension of Solids and Adsorption”, Nauka, Moscow, 1976.
34. *Seo, M., Makino, T., Sato, N.*, *J. Electrochem. Soc.* **133** (1986) 1138.
35. *Morcos, I.*, in “Specialist Periodical Reports Electrochemistry”, Vol 6. In: *Thirsk, H. R.* (Ed.) The Chemical Society, Burlington House, London, (1978), pp. 65–97.
36. *Jaecel, L., Láng, G., Heusler, K. E.*, *Electrochim. Acta* **39** (1994) 1031.
37. *Ibach, H., Bach, C. E., Giesen, M., Grossmann, A.*, *Surf. Sci.* **375** (1997) 107.
38. *Haiss, W.*, *Rep. Prog. Phys.* **64** (2001) 591.
39. *Láng, G. G., Seo, M., Heusler, K. E.*, *J. Solid State Electrochem.* **9** (2005) 347.
40. *Láng, G. G., Ueno, K., Ujvári, M., Seo, M.*, *J. Phys. Chem. B* **104** (2000) 2785.
41. *Láng, G., Heusler, K. E.*, *J. Chem. Soc., Farad. Trans.* **93** (1997) 583.
42. *Láng, G., Heusler, K. E.*, *J. Electroanal. Chem.* **391** (1995) 169.
43. *Láng, G., Heusler, K. E.*, *Russian Journal of Electrochemistry* **31** (1995) 759.
44. *Malpas, R. E., Fredlein, R. A., Bard, A. J.*, *J. Electroanal. Chem.* **98** (1979) 171.
45. *Seo, M., Ueno, K.*, *J. Electrochem. Soc.* **143** (1996) 899.
46. *Ueno, K., Seo, M.*, *J. Electrochem. Soc.* **146** (1999) 1496.
47. *Beck, T. R.*, *J. Phys. Chem.* **73** (1969) 466.
48. *Lin, K. F., Beck, T. R.*, *J. Electrochem. Soc.* **123** (1976) 1145.
49. *Gokhshtein, A. Ya.*, *Elektrokhimiya* **2** (1966) 1318; **4** (1968) 866; **5** (1969) 637.
50. *Gokhshtein, A. Ya.*, *Elektrokhimiya* **6** (1970) 979.
51. *Gokhshtein, A. Ya.*, *Physics-Uspekhi* **43** (2000) 725.
52. *Dickinson, K. M., Hanson, K. E., Fredlein, R. A.*, *Electrochim. Acta* **37** (1992) 139.
53. *Seo, M., Jiang, X. C., Sato, N.*, *J. Electrochem. Soc.* **134** (1987) 3094.
54. *Lin, K. F., Beck, T. R.*, *J. Electrochem. Soc.* **123** (1976) 1146.
55. *Beck, T. R., Beach, K. W.*, in ‘Proceedings of the Symposium on Electrocatalysis’, *Breiter, M. W.*, (Ed.) The Electrochemical Society, Soft-bound Symposium Series, Princeton, N. J., 1974, pp. 357–364.
56. *Horvath, A., Schiller, R.*, *Phys. Chem. Chem. Phys.* **3** (2001) 2662.
57. *G. G. Stoney*, *Proc. Roy. Soc. London* **A32** (1909) 172.
58. *Láng, G. G.*, in ‘Electrochemical Dictionary’, *Bard, A. J., Inzelt, Gy., Scholz, F.* (Eds.), Springer, Berlin, 2008.
59. *Lehmann, V.*, *J. Electrochem. Soc.* **143** (1996) 1313.
60. *Pei, Q., Inganas, O.*, *J. Phys. Chem.* **96** (1992) 10507.
61. *Asaka, K., Oguro, K.*, *J. Electroanal. Chem.* **480** (2000) 186.
62. *Láng, G. G., Ujvári, M., Rokob, T. A., Inzelt, G.*, *Electrochim. Acta* **51** (2006) 1680.
63. *Rokob, T. A., Láng, G. G.*, *Electrochim. Acta* **51** (2005) 93.
64. *Vanhumbeeck, J.-F., Proost, J.*, *ECS Trans.* **2** (2007) 281.
65. *Vanhumbeeck, J.-F., Proost, J.*, *Electrochim. Acta* **53** (2008) 6165.
66. *Láng, G. G., Seo, M.*, *J. Electroanal. Chem.* **490** (2000) 98.
67. *Láng, G. G., Rokob, T. A., Horányi, G.*, *Ultramicroscopy* **104** (2005) 330.
68. *Peterson, J. P., Peterson, R. B.*, *Appl. Optics* **45** (2006) 4916.
69. *Kösters, W.*, Interferenzdoppelprisma für Messzwecke, German patent: 595211, 1934.
70. *Heusler, K. E., Láng, G.*, *Elektrokhimiya* **31** (1995) 826.
71. *Haiss, W., Sass, J. K.*, *J. Electroanal. Chem.* **386** (1995) 267.
72. *Haiss, W., Sass, J. K.*, *J. Electroanal. Chem.* **410** (1996) 119.
73. *Haiss, W., Sass, J. K.*, *Langmuir* **12** (1996) 4311.
74. *Haiss, W., Nichols, R. J.*, *Probe Microscopy* **2** (2001) 77.
75. *Haiss, W., Nichols, R. J., Sass, J. K., Charle, K. P.*, *J. Electroanal. Chem.* **452** (1998) 199.
76. *Binnig, G., Quate, C. F., Gerber, Ch.*, *Phys. Rev. Lett.* **56** (1986) 930.
77. *Bockris, J. O’M., Parry-Jones, R.*, *Nature* **171** (1953) 930.
78. *Bockris, J. O’M., Argade, S. D.*, *J. Chem. Phys.* **50** (1969) 1622.
79. *Bockris, J. O’M., Sen, R. K.*, *Surf. Sci.* **30** (1972) 237.
80. *Voronaeva, T. N., Deryagin, B. V., Kabanov, B. N.*, *Kolloid. Zhurnal (USSR)* **26** (1962) 396.
81. *Bockris, J. O’M.*, in ‘Electrochemistry in Transition’, *Murphy, O. J., Srinivasan, S., Conway, B. E.* (Eds.), Plenum Press, New York, 1992, p. 288.
82. *Teague, E. C.*, *J. Res. Nat. Bur. Stand.* **91** (1986) 171.
83. *Bard, A. J., Faulkner, L. R.*, *Electrochemical Methods*, John Wiley & Sons, New York, 1980, pp. 499–500.

